Journal of Colloid and Interface Science 360 (2011) 471–481

Contents lists available at ScienceDirect

Journal of Colloid and Interface Science

www.elsevier.com/locate/jcis

Preparation and characterization of highly stable lipid nanoparticles with amorphous core of tuneable viscosity

Thomas Delmas [a], Anne-Claude Couffin [a], Pierre Alain Bayle [b], François de Crécy [c], Emmanuelle Neumann [d], Françoise Vinet [a], Michel Bardet [b], Jérôme Bibette [e], Isabelle Texier [a,*]

[a] CEA, LETI-MINATEC, Département des Technologies pour la Biologie et la Santé, 17 rue des Martyrs, F-38054 Grenoble, France
[b] CEA, INAC-SCIB, Laboratoire de Résonances Magnétiques, F-38054 Grenoble, France
[c] CEA, LETI-MINATEC, Département des Technologies, 17 rue des Martyrs, F-38054 Grenoble, France
[d] IBS J.-P. Ebel, UMR 5075 CNRS-CEA-UJF, 41 rue Jules Horowitz, 38027 Grenoble Cedex 1, France
[e] Laboratoire des Colloïdes et Matériaux divisés, ESPCI, 10 rue Vauquelin, 75231 Paris Cedex 5, France

ARTICLE INFO

Article history:
Received 21 February 2011
Accepted 19 April 2011
Available online 28 April 2011

Keywords:
Lipid nanoparticle
Amorphous system
Physical stability
Design of experiments

ABSTRACT

Lipid nanoparticles (LNP) have been designed based on low cost and human-use approved excipients, and manufactured by an easy, robust, and up-scalable process. Fluid colloidal dispersions or gel viscous formulations of highly stable nanoparticles (more than 12 month stability is achieved for some formulations) can be obtained. Their physicochemical properties are studied by Dynamic Light Scattering, Differential Scanning Calorimetry, and NMR. The results picture nanoparticles with a non-crystalline core, which viscosity can be finely tuned by the lipid composition and the temperature. A design of experiments has been used to investigate the limits of the system colloidal stability. The impact of core and surfactant weight fractions have been explored both experimentally and using the design of experiments. The versatility of this physicochemical system could open the way to a wide range of future pharmaceutical applications.

1. Introduction

The use of nanostructured materials is envisioned to revolutionize medical techniques and improve patient care, for instance with earlier and more acute diagnostic, or personalized and controlled therapy [1]. In this context, numerous types of nanocarriers have been proposed to formulate contrast agents or drug mixtures for the intravenous, oral, pulmonary or topical routes [2]. Indeed, nanocarriers can reduce drug systemic toxicity, improve their local distribution and bioavailability, and ultimately control their release kinetics [3].

The most studied delivery systems have historically been liposomes [4], polymeric nanoparticles [5], and lipid nanocarriers such as nanoemulsions [6], Solid Lipid Nanoparticles [7] and lipid-drug conjugates [8]. Lipid-based nanosystems present numerous advantages over other formulations. They are biocompatible, biodegradable and can easily be produced by versatile and up-scalable processes [7]. Nanoemulsions have been studied for a few decades, but these systems suffer from low stability, mostly due to Ostwald ripening or droplet coalescence [9]. In addition, sustained release is difficult to achieve due to the low viscosity of the dispersed phase, which generally results in rapid drug diffusion outside the droplets [10]. New systems, based on solid lipids, namely Solid Lipid Nanoparticles (SLN), have therefore been proposed [7]. However, despite the initial thought that these systems may promote prolonged release of hydrophobic molecules, they show limited controllability [11,12]. Incorporated drugs and lipids forming the nanoparticles usually phase-separate when crystallizing, leading to system instabilities [10,11]. A new type of lipid nanoparticles, nanostructured lipid carriers (NLC), whose core is composed of a mixture of solid and liquid lipids, has therefore been introduced [11]. NLC have been designed to reduce the lipid core crystallinity, responsible for drug expulsion during crystallisation. Three different types of NLC have been described: (i) the imperfect type, whose crystallinity is lowered by creating imperfections in the crystal lattices; (ii) the structureless type, which is solid but amorphous; and (iii) the multiple Oil in Fat in Water (O/F/W) type, in which small droplets of liquid lipids are phase-separated in the solid matrix [11]. The imperfect type (i) has been widely reported [11,13,14], and some studies support the achievement of the two other types (ii) and (iii). Nonetheless, there are discrepancies in the conclusions. For instance, the amorphous state of the core of NLC structureless type (ii) has been consistently demonstrated, whereas the core solid state has been argued [13]. Furthermore, most of the studied

* Corresponding author. Address: CEA, LETI-DTBS, 17 rue des Martyrs, 38054 Grenoble Cedex 9, France. Fax: +33 438 785 787.
E-mail address: isabelle.texier-nogues@cea.fr (I. Texier).

0021-9797/$ - see front matter © 2011 Elsevier Inc. All rights reserved.
doi:10.1016/j.jcis.2011.04.080

systems crystallise after a few hours, days, or rarely months [13]. The structure of the multiple O/F/W type (iii) also leads to debate. Different studies of the same system led some authors to the conclusion that the oil phase is partially segregated within the solid fat nanoparticles [15], whereas others conclude that the liquid oil is completely demixed and only attached to the fat solid particles rather than encapsulated inside, in the so-called 'nanospoon structure' [16].

Along the work on nanocarrier intrinsic properties improvement, a significant effort on the galenic of lipid formulations has been done [17,18]. SLN and NLC have been generally produced by high pressure homogenization [7,19]. Such a process is efficient in producing 100–200 nm diameter particles and has the advantage of being easily up-scalable for industrial production [7,19]. However, one historical major drawback of such a manufacturing process is that it commonly produces diluted dispersions, whereas total lipid concentrations from 20% to 40% w/w are highly desirable to turn low viscous solutions into elastic gels, adopting classical dermal preparation viscoelastic properties for cosmetic and pharmaceutical applications [20]. Getting gel-like formulations generally requires a multistep procedure which combines first the production and then one or more additional steps conferring gel-like behaviour to the dispersion. It can be achieved by addition of viscosity enhancers, such as long chain polyoxyethylene polymers, or by re-concentrating the dispersion through ultrafiltration. A one-step approach for the design of a gel of crystalline core lipid particles processed by high pressure homogenization has yet been proposed and is seen to produce stable semisolid SLN dispersions with typical average diameters of 150–300 nm [18].

In this context, we present very stable amorphous lipid nanoparticles, abbreviated as LNP in text, whose intra- and inter-particle viscosities can be controlled. In comparison to previously described lipid nanosystems, we previously demonstrated that the presence of complex mixtures of long chain glycerides in the internal phase induces LNP formulations displaying long-term colloidal stability due to the prevention of Ostwald ripening, coalescence being minimized for nanometric sized emulsions [21]. It is here evidenced that the use of complex mixtures of long chain glycerides also allows the fine tuning of the LNP core viscosity as a function of composition and temperature, promotes the amorphicity of the lipid phase, and allows the system to be extremely stable as an aqueous dispersion. The present paper is focussed on the physicochemical investigation of this lipid-based nanosystem, as well as its formulation potentialities. Moreover, the use of ultrasonication as a manufacturing process is demonstrated to avoid the need of a multistep procedure to obtain gel-like formulations as well as perfectly liquid dispersions. In addition, ultrasonication has been shown to be more efficient in obtaining smaller nanoparticle diameters while consuming less energy than currently used high pressure homogenization techniques [22]. Such small diameters are important to obtain original rheological properties: decreasing nanoparticle size leads, for instance, to a dramatic increase of the gel structure strength [23]. These new formulations should therefore open up new opportunities as dosage forms for parenteral and topical delivery routes (lotions, creams...), but also for the preparation of capsules or implants.

2. Materials and methods

2.1. Materials

Suppocire NC™ is a kind gift from Gattefossé (Saint-Priest, France). Myrj s40™, Myrj s50™, Myrj s100™ (polyethylene glycol 40, 50 or 100 stearate, respectively) and Super-refined Soybean oil™ are kindly donated by CRODA (Chocques, France). Polyethylene 35 and 80 stearate are similarly donated by Stearinerie Dubois (Boulogne Billancourt, France). Lipoid s75™ is purchased from Lipoid (Ludwigshaffen, Germany), other chemical products from Sigma Aldrich (Saint-Quentin Fallavier, France).

2.2. LNP fabrication process

The lipid phase is prepared by mixing solid (Suppocire NC™) and/or liquid (Super-refined Soybean oil™) glycerides and the lipophilic surfactant Lipoid s75™, while the aqueous phase is composed of the hydrophilic surfactant, Myrj s50™ for instance, in 1X PBS aqueous buffer (100 mM phosphate, NaCl 154 mM, pH 7.4). After homogenization at 45 °C, both phases are crudely mixed and sonication cycles are performed at 45 °C during 5 min. Nonencapsulated components are separated from LNP by dialysis (1X PBS, MWCO: 12 kDa, overnight). Prior to characterization, LNP dispersions are filtered through a 0.22 μm cellulose Millipore membrane. In a typical experiment, particles are composed of 15.2% (w/w) of lipid phase (with a lecithin/PEG surfactant weight ratio of 0.44 and a surfactants/core weight ratio of 1.64) and 84.8% (w/w) aqueous phase composed of 13.6% (w/w) Myrj s50™ in 1X PBS. This composition leads to 45-nm diameter particle dispersion. Other compositions with different lecithin/PEG surfactant weight ratio or surfactants/core weight ratio have been explored, as will be detailed in Section 3. Different wax/oil ratios (w/w) in the core have been used. For simplification, LNP samples are quoted NCXX where XX defines LNP core composition by the weight ratio of wax (% w/w).

2.3. Cryo-Transmission Electron Microscopy (TEM)

Cryo-TEM analysis is performed using a CM200 microscope (FEI Eindhoven, The Netherlands) with a LaB_6 electron source operating at 200 kV. The sample is deposited onto a holey carbon grid, blotted to remove excess liquid, and frozen by plunging rapidly into liquid ethane at the temperature of liquid nitrogen. Grids are transferred to a Gatan 626 cryoholder and imaged by low-dose techniques, maintaining the low temperature throughout (−185 °C). Images are recorded at a nominal magnification of 38,000×. Micrographs are recorded on Kodak SO-163 film and are developed for 12 min in full-strength Kodak D19.

2.4. Dynamic Light Scattering (DLS)

The hydrodynamic diameter and zeta potential of the lipid nanoparticles are measured with a Malvern Zeta Sizer Nanoinstrument (NanoZS, Malvern, UK) in 0.1X PBS buffer. LNP physical stability is investigated by DLS measurements over 4 months for samples stored at room temperature (22 ± 2 °C). At least three different LNP batches (2 mL, lipid dispersed phase weight fraction: 10%) are used per condition. Mean average diameters and polydispersity indices reported are issued from scattered light intensity results. Data are expressed in terms of mean and standard deviation of all the samples for each condition, each sample result being the mean of three independent measurements performed at 25 °C.

2.5. Differential Scanning Calorimetry (DSC)

DSC thermograms are recorded on a TA Q200 system (TA instrument, France). Samples of 2–5 mg of bulk material or 10–20 mg LNP dispersion are filled into standard aluminium sample pans (TA instruments, France), and an empty pan is used as a reference. Heating curves are recorded at a rate of 10 K/min over the temperature range 20–80 °C. Measurements are performed immediately after preparation and after 4 months storage at room temperature or 4 °C.

2.6. ^{1}H NMR spectrometry

^{1}H NMR spectra of LNP are recorded at 10 °C, 25 °C and 35 °C using a Bruker Avance DPX 500 spectrometer (Bruker, Germany), operating at 500 MHz for proton. Both 1D and 2D NMR experiments are performed using the standard Bruker pulse sequences. Data are generally further processed and analysed with the MestRe-C v3.0 software. 3-(Trimethylsilyl)-1-propanesulfonic acid sodium salt (DSS), for D_2O dispersions, or tetramethylsilane (TMS), for $CDCl_3$ dispersions, are added as 0 ppm reference. An aliquot of each LNP aqueous dispersion is filled in an NMR tube and accurately weighted quantities of 0.1% w/w DSS in deuterated water (or 0.1% w/w TMS in chloroform) are added. The assignment of the ^{1}H resonances of PEG-40-stearate (Myrj s40™), lecithin and glycerides mixtures (soybean oil and Suppocire NC™) as pristine commercial ingredients is done by classical 1D and 2D methods such as ^{1}H–^{1}H homonuclear COSY and NOESY [24].

2.7. Design of experiments

A design of experiments based on a mixture design with main effects and interactions is used to study the physicochemical behaviour of the LNP formulations (Design Expert 07 software®). Four factors completely describing the LNP system for a defined core composition are investigated: aqueous buffer weight fraction (X_1), lipid mixture weight fraction (X_2), lipophilic surfactant and hydrophilic surfactant weight fractions (respectively noted X_3 and X_4). Using our previous lipid nanosystem expertise, limits are imposed to the explored experimental domain in order to investigate relevant nanoemulsion domain. Two quantitative parameter responses are studied: the LNP particle diameter (Y_1) and polydispersity (Y_2). Both can be experimentally measured by DLS measurement. The initial design has been based on a D-optimal construct. Mixture models with main effects and interactions are hypothesized to describe the relationships between the responses Y_1 and Y_2 and the studied factors X_1, X_2, X_3 and X_4:

$$\begin{cases} Y_i = a_0 + \sum a_i X_i + \sum a_{ij} X_i X_j \\ \sum X_i = 1 \end{cases}$$

Optimal points selection is performed by the Design Expert software® and leads to the construction of an initial 32 experiments design. However, further trials are added to improve the model accuracy (repetition of most influent points/addition of complementary formulation trials). Finally, 82 trials are used to model the two quantitative parameter responses: particle diameter (Y_1) and emulsion polydispersity (Y_2). The design of experiments description is summarized in Fig. 8. In practice, 2 g LNP dispersions are used for this study and composition is changed to study the effect of each considered factor, using the 75%/25% w/w wax/oil mixture as internal oily phase. The model coefficients are then estimated by a multiple regression analysis based on a least-squares estimation technique implemented with the Design Expert 07 software®.

3. Results and discussion

3.1. Choice of LNP ingredients

The LNP composition is pictured in Fig. 1. All components are FDA approved, and already clinically used for diverse applications, meaning their GMP purity is suitable with industrial development in the pharmaceutical field. A vegetable oil for the core (soybean oil) and a phospholipid surfactant for the membrane (phosphatidylcholine) are chosen for their acknowledged biocompatibility. Moreover, soybean oil and semi-synthetic wax (Suppocire NC™) are composed of saturated and unsaturated long-chain triglycerides (saturated C_{12}–C_{18} for Suppocire and unsaturated C_{16}–C_{18} for soybean oil), limiting therefore the oil solubility in the continuous phase through mass transfer. This fact, in addition to the dialysis step, which eliminates surfactants and eventual lipids solubilised in the continuous aqueous phase, limit possible destabilisation of the colloidal dispersion through Ostwald ripening [21]. In addition, having an oil/wax mixture in the core provides an opportunity to modulate the particle internal physical state, as will be demonstrated below, and therefore potentially the associated encapsulation and release properties of molecules of interest that could be entrapped in the LNP. Finally, the hydrophilic co-surfactant is chosen among PEGylated stearates, aiming for a steric barrier preventing coalescence and favouring small particle diameter, as will be evidenced below. Moreover, PEG chains are known to provide a stealth character to the nanocarriers and slow their elimination from the bloodstream whenever the intravenous route is envisioned.

The LNP ingredient choice is crucial if aiming to biomedical applications, since two main characteristics of the nanocarrier need to be fulfilled: (1) it needs to be non-toxic and biocompatible, further biodegradability of the nanocarrier can be an advantage; (2) it needs to present a long-term colloidal stability under storage conditions, even though additional treatment, such as lyophilisation, can sometimes be used to produce sufficiently stable products [19]. These are the minima required to envision industrial applications in the biopharmaceutical field. The LNP composition fulfils these requirements.

The biocompatibility mostly relies on that of each component forming the nanocarrier, even though some specific effects can arise from the nanometer scale of the product [25]. Lipid-based formulations are generally preferred because of the structural similarities between their components and those of cell membranes, allowing the reduction of toxicity risks from excipients. Lipids and surfactants entering the LNP composition are chosen among a list of high purity excipients commercially available for pharmaceutical formulations (low cost and easily available) [26].

Considering the long-term colloidal stability objective, lipid nanoparticle dispersions are prone to both Ostwald ripening and coalescence destabilisation phenomena [21]. Preliminary studies have allowed the understanding of the fundamentals of nanoemulsion stability, and the critical importance of parameters such as the oil solubility in the continuous phase or the membrane rigidity. We previously demonstrated that wax addition in the LNP lipid oily core efficiently prevents Ostwald ripening [21]. Similarly, using a combination of surfactants and co-surfactants at the membrane is known to favour protection against both Ostwald ripening and coalescence [21].

For applications necessitating parenteral injection, further additional specifications need to be fulfilled. Such administration route requires nanocarriers avoiding recognition by the immune system and presenting prolonged blood circulation [26]. Interfacial properties are critical for that purpose: nanoparticle diameter and surface charge, but also surface topology and porosity have been shown to dramatically affect nanoparticle/biological media interactions, and dictate their *in vivo* fate [27]. Neutral coating is to be preferred and long chain hydrophilic polymer coatings, such as PEG chains, are efficiently used as a steric barrier for that purpose [26,28,29]. Moreover, PEGylated surfactants are known to improve the furtivity of nanocarriers because they both favour their colloidal stability [21] and reduce their binding by opsonins and their macrophage uptake [29]. Finally, the composition of the internal phase has also been shown to alter biodistribution of lipid emulsions [29]. Medium-chain triglycerides-based formulations (MCT) are for instance cleared more quickly than their long-chain triglycerides (LCT) counterparts. This relies on different

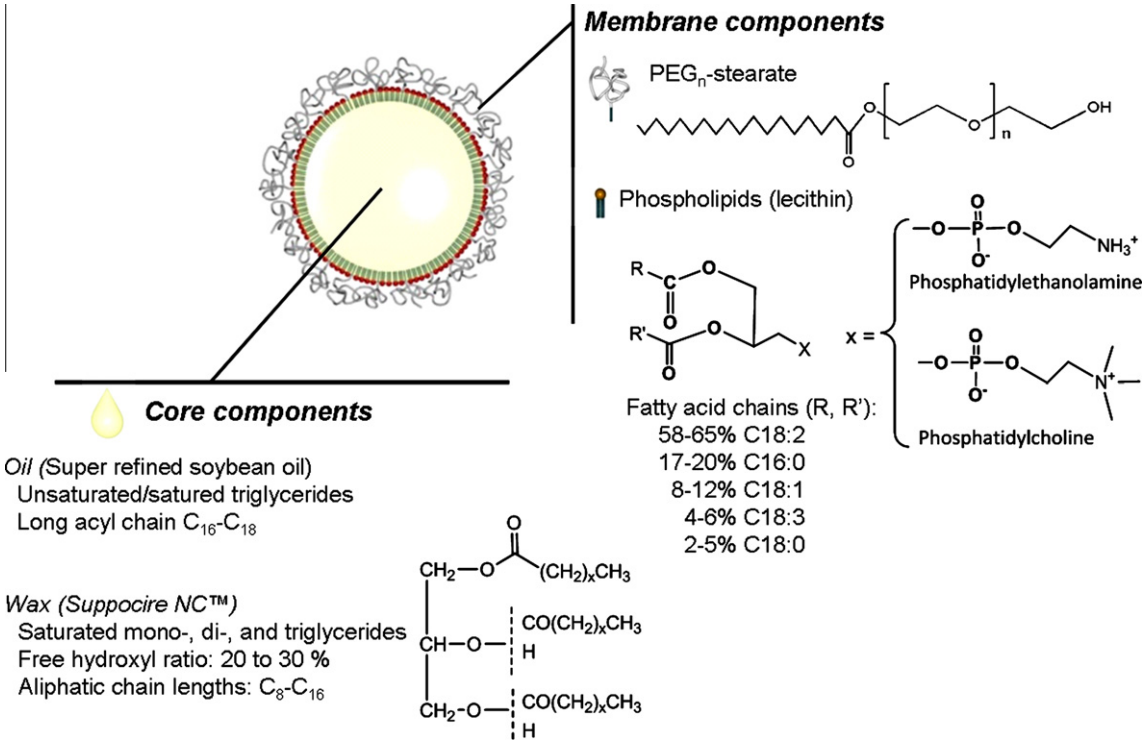

Fig. 1. LNP schematic representation. Molecular structure of the core and membrane components incorporated in the preparation of LNP.

degradation rates through hepatic and endothelial lipase degradation [29]. Core lipids with long-chain triglycerides entering the LNP composition should present slow *in vivo* clearance rate [29].

3.2. LNP processing and influence of the continuous phase weight fraction

We previously reported a detailed study on the LNP sonication process and parameters governing its kinetics [21]. We here highlight that sonication allows the one-pot processing of LNP formulations with tuneable viscosities, ranging from highly diluted liquid-like suspensions to highly concentrated gel-like formulations without addition of any viscosity enhancers (Fig. 2). The viscosity is here mainly tuned by the continuous phase weight fraction of the formulation. This is of particular interest to propose a panel of dosage forms for diverse applications such as injectable fluids (liquid-like form) or implants (gel-like form). Interestingly, increasing the dispersion viscosity (from 0.5% to 40% w/w of lipids) does not affect nanoparticle stability, which can be as long as more than 12 months at 40 °C for optimized formulations (Fig. S1 in Supplementary information and [30]).

Contrary to microemulsions which spontaneously self-assemble and are thermodynamically stable, the formation of nanoemulsions requires the input of energy in order to overcome the oil/water interfacial tension that exists in these systems [9,21]. Different emulsification processes have been described for the production of lipid nanoemulsions, SLN or LNC. Low-energy processes, such as Phase Inverse Temperature (PIT), or Catastrophic Phase Inversion (CPI), are advantageous for the encapsulation of labile drugs and macromolecules, but are highly dependent on the formulation composition [19]. High-energy methods encompass mainly high pressure homogenization and sonication [19]. One advantage of sonication, however not widely used, is the fact that low volume highly viscous solutions can be processed easily. It is also a robust, up-scalable and easy-to-implement industrial process. Sonication also provides the sufficient shear rates to achieve particle sizes as low as 30–35 nm diameter, as measured by DLS and confirmed by cryo-TEM (Fig. 2) [21]. This is also noticeable, since larger diameters are usually reported for NLC, processed by high pressure homogenization [8,19].

Therefore the LNP system described herein displays original colloidal properties for a lipid-based nanoemulsion: small particle diameter, associated with an excellent colloidal stability (in storage conditions of 4–40 °C range), and the possibility to be processed in concentrated formulations. In order to further understand the origin of such physicochemical properties, the influence of the particle core and shell composition is here carefully studied, and further characterizations are undertaken.

3.3. Influence of the core composition

Core composition and the associated internal physical state are critical when considering physicochemical characteristics such as physical stability, and encapsulation/release behaviours of lipid nanoparticles. It is therefore important to fully characterize and understand the physicochemical properties associated with the different compositions of a lipid system. LNP hydrodynamic diameter and zeta potential are measured using Dynamic Light Scattering (DLS). To gain insight into the lipid core crystallinity, particle internal physical state is further investigated by Differential Scanning Calorimetry (DSC), whereas ^{1}H NMR spectrometry is used to assess lipid core internal viscosity.

3.3.1. Particle size and surface charge

Modifying LNP internal composition is seen to slightly affect particle size (Fig. 3): average hydrodynamic diameter of LNP decreases when increasing the wax content, while all other ingredient concentrations are kept constant (Fig. 3). Meanwhile, LNP surface charge is unaffected since the zeta potential remains constant with values close to – 5 mV (Fig. 3). This is expected since the surface charge is due to the chemical structure of the interface, which is not modified when modulating the LNP core composition.

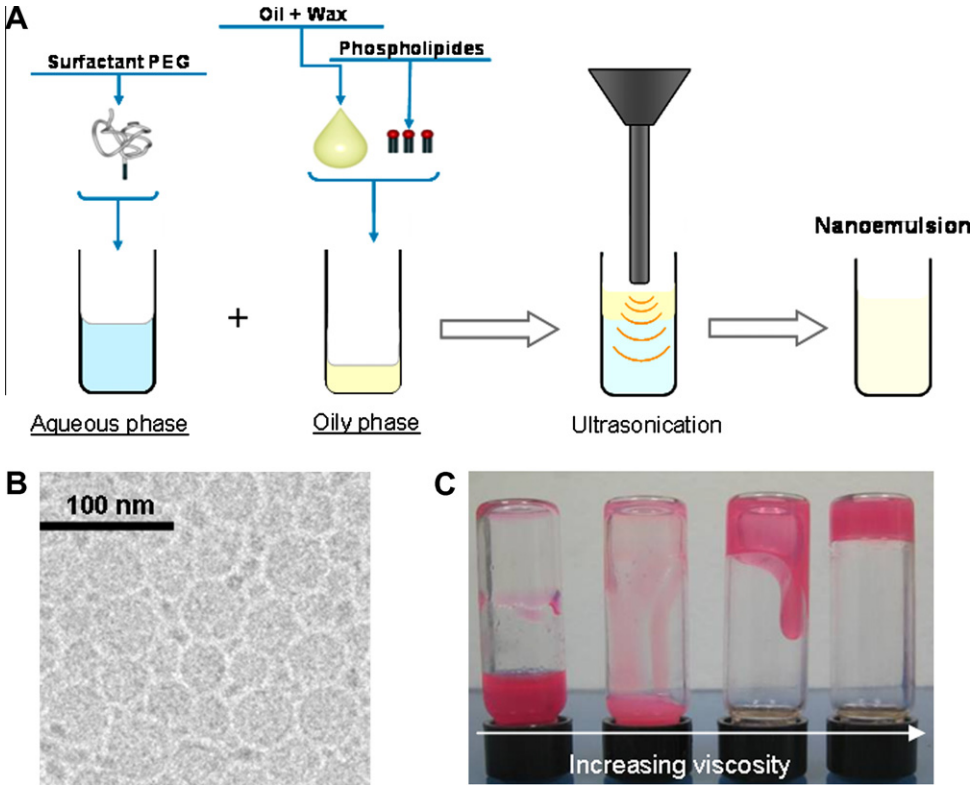

Fig. 2. LNP manufacturing process leading to nanometric particles dispersed in formulations of tuneable viscosity. (A) Scheme depicting the LNP manufacturing process. (B) Cryo-TEM photograph of 50 nm diameter LNP. Formulation used: 340 mg NC75; 65 mg Lipoid s75; 345 mg Myrj s40; 1250 μL 1X PBS. (C) Photograph of samples with different viscosities after 1 min flask inversion. The lipid dispersed phase weight fraction governs the sample viscosity: from highly diluted particle suspension (left) to gel-like behaviour (right) (for visualization convenience, Nile red loaded formulations have been used). Formulation used: 340 mg NC75; 65 mg Lipoid s75; 345 mg Myrj s40; respectively from left to right *X* = 2050, 1750, 1050, or 850 μL 1X PBS.

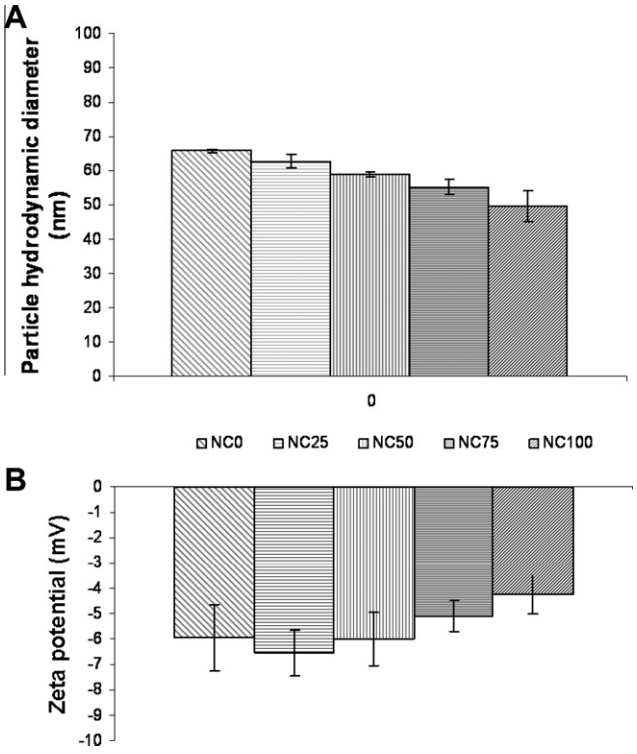

Fig. 3. Influence of the lipid core composition on the LNP mean hydrodynamic diameter (A) and zeta potential (B). Formulations used: 340 mg NCXX; 65 mg Lipoid s75; 345 mg Myrj s40; 1250 μL 1X PBS (XX defining the% of wax in the core (w/w)).

Emulsion size is the result of two opposite processes: droplet break up and coalescence [21]. In turbulent shear, droplets break-up is mainly governed by the shear rate, surfactant type/concentration and the relative viscosities of the two phases. Meanwhile, during the emulsification process, coalescence mostly relies on surfactant type/concentration and continuous phase viscosity [21,31]. When modifying the LNP core wax/oil ratio composition, all process conditions are similar except the viscosity of the internal phase. It is therefore most likely that the slight difference in nanoemulsion diameter is due to the difference in relative viscosities between dispersed and internal phases. Droplet break-up is most efficient, and the droplet diameter lower, when the dispersed/continuous phase viscosity ratio (n_D/n_C) is comprised between 0.1 and 5, since it promotes a good shearing efficiency while optimizing the homogenization process [21]. The fact that oil and wax, and therefore their mixture at different ratio, present different viscosities, even at the bath temperature of 45 °C, should account for the observed differences in LNP diameter displayed in Fig. 3.

3.3.2. Core crystallinity

Among other parameters, crystallinity of the lipid phase has been shown to dramatically affect lipid nanoemulsion physical stability, as well as their encapsulation/release properties. LNP core crystallinity has been investigated over 4 months by DSC analysis. The 50 nm-diameter particles with different oil/wax core compositions have been analyzed just after their preparation and after 4-month storage at room temperature (22 ± 2 °C). The thermograms are displayed in Fig. 4, and compared to those of the bulk dispersed phases (i.e. the non-formulated lipid mixtures).

Suppocire NC™ (NC100 bulk) is a semi-crystalline solid at room temperature, since DSC thermogram presents an important

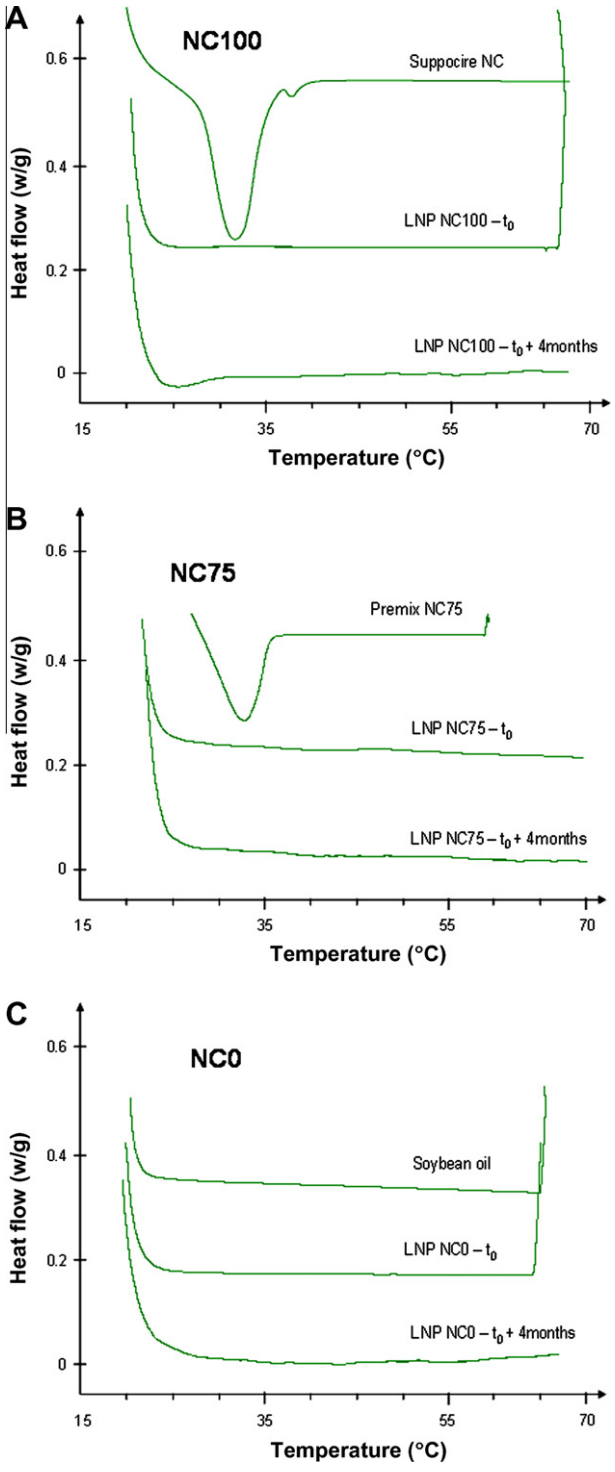

Fig. 4. DSC thermograms. Thermograms obtained for LNP with different core composition 1 day (t0) and 4 months (t0 + 4 months) after their preparation and storage at 22 ± 2 °C, are compared with those obtained with the bulk phases of similar composition (A. NC100: 100% wax; B. NC75: 75% wax/25% oil; C. NC0: 100% oil). Formulations used: 340 mg NCXX; 65 mg Lipoid s75; 228 mg Myrj s40; 1250 μL 1X PBS.

endothermic peak at 30–35 °C, assigned to the fusion of crystalline network (Fig. 4A). Soybean oil (NC0 bulk) does not display any thermal event when heated from room temperature since this material is liquid at this temperature (Fig. 4C). Nonetheless, it undergoes a partial crystallization when cooled below 10 °C (data not shown). As a lipid mixture of 75% wax and 25% oil, the NC75 bulk phase presents a fusion peak of intermediate intensity around 30–35 °C (Fig. 4B). Once nanoformulated and right after LNP preparation, no thermal event is observed when heating from 20 °C to 80 °C for all the lipid phases (NC0, NC75, NC100), whatever the content of the wax/oil mixtures. Similar results are obtained after 4-month storage at room temperature or at 4 °C. This suggests that the lipid phases, when LNP formulated, do not crystallize even for pure wax composition stored at 4 °C, over the 4-month investigated period: the lipid core could be considered to be in an amorphous state.

Upon cooling, lipid nanoparticle cores usually solidify by crystallization, as does the bulk phase of same composition. However, because of the Kelvin effect (i.e. the decrease of probability to have nucleants in the particle core whenever its diameter decreases), and also due to the increased importance of surface effects, supercooling has been widely reported for lipid nanodroplets in comparison to the bulk phases [13]. Incorporation of liquid lipids in the solid matrix has lead to less perfect crystalline structures favouring this supercooling effect, but lipid core crystallization remains the rule [13]. For instance, monoacid triglycerides nanoparticles (trilaurin – C_{12}/trimyristin – C_{14}) can either be kept in a supercooled liquid state at room temperature, or forced to crystallize by 4 °C cooling [13].

The high complexity of the lipid mixture entering the LNP composition could account for their resistance to crystallization and their supercooling effect. When increasing the wax content of the LNP core, the chemical heterogeneity of the lipid phase is further dramatically increased, hindering ordering through crystallisation. Indeed, Suppocire NC™ is a complex mixture of mono- di- and triglycerides of various acyl chain lengths (C_8–C_{18}), with an overall hydroxyl value of 20–30% (Fig. 1). Short acyl chain lengths are known to disfavour crystallisation, presenting more free ends enabling to move. In addition, a high hydroxyl value, corresponding to a high amount of partial glycerides, generally leads to less crystalline material, as previously reported [32]. In addition, unsaturated alkyl chains present in soybean oil tend to disfavour ordering by double-bond blocked cis/trans conformations [33].

The lipid core crystallinity can strongly impact the overall colloidal stability of lipid droplet formulations, possibly leading ultimately to irreversible gelation of the dispersion [34]. Indeed, when crystallising, the previous random isotropic organisation of the lipids inside the nanoparticle, which favours spheroid shapes, is quickly changed into well-organised mono-oriented platelets [34]. This change in nanoparticle morphology is generally associated with an increase in surface area (the sphere being the shape giving the less interface area for a given volume). As a consequence, surfactant coverage is dramatically decreased, if free surfactants are not available in solution [34]. This favours irreversible inter-particle contact (i.e. aggregation), until forming a gel in place of the previously liquid dispersion. Core crystallinity has also been linked to the encapsulation and release properties of drugs incorporated into lipid nanoparticles. The raise in the lipid ordering upon crystallization leads to phase separation between the solvent lipid phase and the encapsulated molecules [10,35]. As these molecules cannot be integrated in the new well-ordered lipid phase, they are generally expelled outside the nanoparticles, being adsorbed on their surfaces, or released as free aggregates in solution [11]. This dramatically reduces the effective drug payload and the associated release behaviours.

The long-term core amorphicity observed for the LNP is therefore a key factor for future applications of these new lipid nanosystems, as smart carriers for the entrapment of therapeutic or diagnostic agents. The absence of core crystallinity also seems to categorize wax core containing LNP described herein in the structureless type (ii) of NLC depicted in the introduction [11]. Further characterization of the LNP core physical state is thus pursued to

assess the LNP core viscosity and complete the knowledge on the lipid nanosystem.

3.3.3. Core viscosity

^{1}H NMR spectroscopy can be efficiently used to gain information on molecular mobility and consequently on material viscosity [36,37]. Indeed, in liquid-state NMR, for molecular systems with reduced mobility, signal broadening may be observed, when the extreme narrowing conditions are not fulfilled. In the extreme limit for a completely solid matrix, no signal is expected to appear in spectra recorded under liquid-state ^{1}H NMR conditions, as already observed for solid nanomatrixes [38]. The influence of the core composition and temperature on LNP internal viscosity can therefore be investigated by liquid ^{1}H NMR analysis in a qualitative way (Fig. 5).

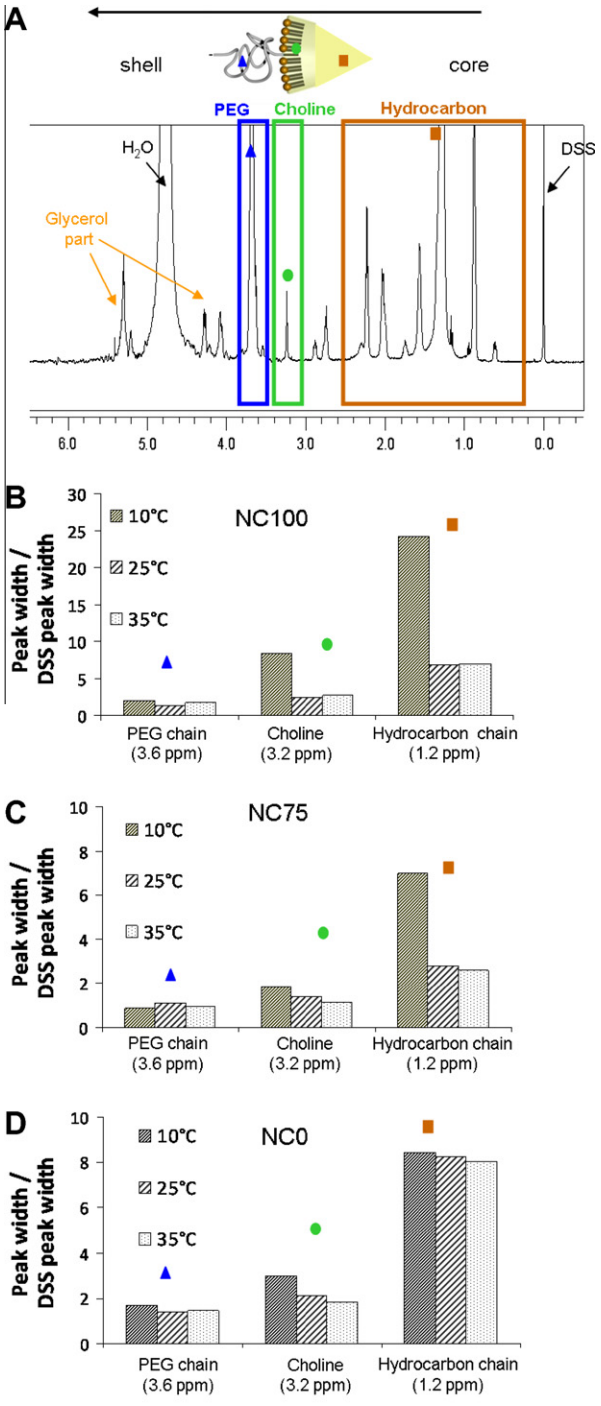

Fig. 5. ^{1}H NMR characterization: (A) ^{1}H NMR spectrum of 50 nm diameter LNP NC75 (75% wax/25% oil in the core) at 35 °C; (B–D) width of characteristic peaks as a function of temperature (10 °C, 25 °C and 35 °C) for various core composition (B. NC100: 100% wax; C. NC75: 75% wax/25% oil; C. NC0: 100% oil). Fifty nanometer diameter formulations used: 340 mg NCXX; 65 mg Lipoid s75; 228 mg Myrj s40; 1250 μL 1X PBS.

As the chemical structures of the LNP lipid components (oil/wax/phospholipid/PEG surfactant) are very alike, strong overlapping of their NMR signals are expected and as a matter of fact observed. However, a complete analysis of the proton spectra has allowed the unambiguous assignment of specific NMR signals of the LNP ^{1}H NMR spectra to the following components: fatty acid-bearing long alkyl chains, ethylene glycol of PEG surfactant, and glycerol-based moiety. These main resonance regions, as shown in the LNP ^{1}H NMR spectra of Fig. 5A, are the following: (i) the resonances located in the 0.5–2.8 ppm range, reflecting to the methyl protons of the saturated aliphatic chains; (ii) the resonances located in the 3.0–5.0 ppm range attributed to the protons of CH, CH_2, CH_3 groups belonging to glycerol, ethylene glycol (PEG) and choline/ethanolamine moieties; and (iii) in the 5.0–6.0 ppm region, for which signals of methine protons owing to trigliceridyl moiety and unsaturated fatty acid chains (linoleic and oleic chains included in soybean oil and lecithin surfactant) are detected. Moreover, three specific signals (labelled by different symbols) can be confidently detected to follow the behaviour of each portion of the nanoparticles. The resonance at 3.6 ppm, (triangle symbol in Fig. 5A), can mainly be associated to the methylene protons of the ethylene glycol units of PEG surfactants. This signal can be used to characterize the behaviour of the outer layer of the nanoparticle shell. The methyl protons bearing by the trimethyl ammonium groups of the choline moiety within the lecithin molecules appear as a specific singlet signal located at 3.2 ppm (circle symbol in Fig. 5A). Through this signal, the behaviour of the inner nanoparticle shell can be investigated. Finally, the signal (square symbol) at 1.26–1.29 ppm lies in the resonance range of protons of CH_2 groups of fatty acid chains, with length ranging from C_8 up to C_{18}, and is representative to the hydrophobic block of the whole LNP components. However, because core components are preponderant in weight and possess numerous aliphatic chains per molecule, this peak overall behaviour shall mainly reflect core internal state.

The width of the three peaks representative of particle locations is measured at three temperature conditions (10 °C, 25 °C and 35 °C) for three wax/soybean oil ratios (NC0, NC75, NC100) (Fig. 5B–D). Whatever core composition and temperature, the width related to PEG chain peaks undergoes no influence. This feature is in agreement with the fact that this hydrophilic block composing the external membrane of LNP is exposed to aqueous environment. PEG chains should present similar mobilities for all temperatures explored. Similar trends are observed for trimethyl ammonium groups (3.2 ppm) of choline moiety (Fig. 5B–D) and methylene protons (2.9 ppm) of ethanolamine moiety (data not shown) as polar head of phospholipids. On the contrary, integration of aliphatic chains (1.2 ppm) is subject to change with temperature, depending on LNP core composition. When internal core is composed only of soybean oil, no evolution is noticed (Fig. 5D). While adding wax in core composition, the peak of this proton groups broadens with decreasing temperature, indicating aliphatic chain molecular mobility decrease. This suggests that below melting point temperature of wax (25–35 °C as illustrated in Fig. 4) and in particular at 10 °C, internal viscosity dramatically increases without formation of crystalline state (as previously demonstrated by DSC study and depicted in Fig. 4).

These results evidence the controllability in the LNP core viscosity brought by temperature or lipid core composition effects. It was previously reported that lipid nanoparticle core composition

clearly affects the internal physical state of the oily phase: from liquid state for classical emulsions composed of Medium Chain Triglycerides (MCT) or other low molecular weight compounds, to more viscous state upon addition of long-chain triglycerides (LCT) or other high molecular weight lipid chains [15], or even to crystalline solid state commonly observed for SLN composed of simple glycerides [7]. Interestingly, this physical state has been demonstrated to dramatically affect physical stability, but also encapsulation and release properties. Liquid dispersions, such as classical nanoemulsions, generally suffer from stability issues, due to material leakage through the continuous phase, favouring high Ostwald ripening rates [21]. Conversely, SLN suffer from gelation issues following crystallisation of the lipid phase [34]. These features have been correlated to high differences in encapsulation and release behaviours [10]. Nanoemulsions are for instance seen to present high loading efficiency, but often suffer from leakage issues, being unable to retain encapsulated molecules under storage [10]. Conversely, SLN, while presenting interesting loading efficiencies, often undergo high drug expulsion when crystallisation of the lipid phase [11]. From ^{1}H NMR and DSC experiments, we can depict the LNP as amorphous-core lipid nanoparticles, in which core viscosity can be tuned to desired applications. Achieving controllable kinetics of payload release using this new nanosystem therefore appears as a realistic promise. LNP appear very similar to the already described structureless type (ii) NLC [11]. However, contrarily to other previously described lipid nanosystems [14,26], a wider range of particle diameters (30–200 nm) and formulation viscosities (Fig. 2), and most important, a far increased long-term stability (Fig. S1) are achieved thanks to the LNP manufacturing process and their specific core, but also interface composition, as detailed below.

3.4. Influence of the interface ingredient proportion

For a defined set of lipid core composition, as well as lecithin and PEG-stearate surfactant molecular ratios, Fig. 6 depicts the influence of the PEG chain length of the PEG-stearate surfactant on the average LNP diameter. For intermediate PEG chain length ($20 \leqslant$ ethylene glycol units (n_{PEG}) $\leqslant 50$), no real effect on particle diameters is obtained and LNP dispersions present similar particle size distributions. Increasing the length of the PEG chain above 50 ethylene glycol units, leads to relevant particle size increase. When PEG-stearate surfactant with chain smaller than 20 ethylene glycol units are used, numerous formulation issues are generally encountered. The most frequent issue is related to foam formation, but sample inhomogeneity can sometimes be predominant. Foam formation has been accounted for by too fast energy input, and the associated quick kinetics of diameter decrease during the fabrication process [21]. Such problem could be avoided by decreasing the sample temperature, using a cooling bath, while increasing its viscosity, by addition of viscosity enhancers such as glycerol [21]. The increase of the hydrodynamic particle diameter in solution for $n_{EG} > 50$ could be accounted for by a change of PEG conformation and/or surface tension γ. Indeed, whereas macroscopic soybean oil/PBS surface tension are quite similar for short PEG chain lengths ($20 \leqslant n_{PEG} \leqslant 50$ leads to $3.10 \pm 0.15 \leqslant \gamma$ (mN m^{-1}) $\leqslant 3.58 \pm 0.36$), a significant increase is observed for longer PEG chains ($n_{PEG} = 100$ leads to a surface tension of 4.71 ± 0.36 mN m^{-1}). Even if these values are macroscopic surface tensions obtained by pending drop measurements, which might be slightly different from the nanoscopic surface tensions at the nanoparticle/solution interface, they reflect a trend evolution for the interfacial tension γ [21]. Overall, intermediate PEG chain lengths ($20 \leqslant n_{PEG} \leqslant 50$) appear as a good compromise between formulation issues and the achievement of large size particles which might not be appropriate for *in vivo* use. Moreover, it is now well established that PEG coating with molecular weights superior to 1000 g mol^{-1} ($n_{PEG} \geqslant 20$) are sufficient to efficiently prevent non-specific surface protein adsorption, undesirable feature for biological applications [28].

The impact on the hydrodynamic diameter of the droplets of the total (lecithin + PEG-stearate) surfactant concentration and the PEG-stearate/lecithin ratio are displayed in Fig. 7. This study is carried out using PEG surfactant with 2000 g mol^{-1} molecular weight (Myrj s40™, 40 ethylene glycol motifs). Increasing the PEG surfactant concentration (A1 axis) or the lecithin concentration (A2 axis), while keeping the other surfactant concentrations at constant levels, significantly reduces the obtained LNP particle diameter. Nonetheless, contrary to the PEG surfactant, the exclusive use of lecithin, even in high quantities (from 25 mg to more than 200 mg, data not shown), does not allow to obtain droplets of size below 200 nm, and all obtained populations present a high polydispersity index (PDI > 0.25). As expected, increasing the total surfactant concentration for a given lecithin/PEG surfactant (Myrj s40™) ratio: 0.5 w/w, A3 axis in Fig. 7) also decreases progressively the LNP diameter. Finally, when looking at the evolution of the diameter while varying the lecithin/PEG ratio surfactant at a constant total mass of surfactants (A4 axis), a synergic effect between the two surfactants can be highlighted. Indeed, smaller particle diameters are obtained when mixing both hydrophilic and lipophilic surfactants instead of using one surfactant alone (A4 axis).

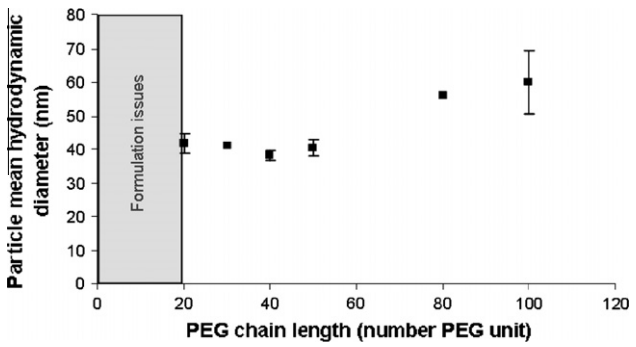

Fig. 6. Influence of the PEG surfactant chain length on the LNP mean hydrodynamic diameter. Formulations used: 200 mg NC75; 100 mg Lipoids75; 0.1 mmol PEG surfactant; 50 mg glycerol in 2.9 mL 1X PBS. Results are given as mean and standard deviation over three independent samples per condition.

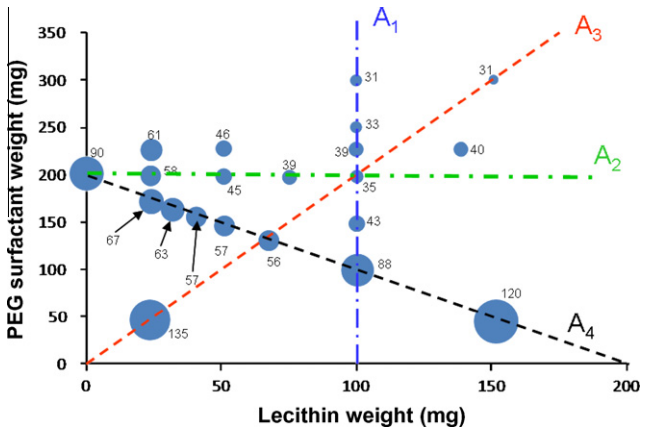

Fig. 7. Influence of the surfactant shell composition on the LNP mean hydrodynamic diameter (nm), reflected by the circle diameter and indicated value. Formulations used: 200 mg NC75; X mg Myrj s40; Y mg Lipoid s75; 50 mg glycerol in 1.45 mL 1X PBS. Results are given as average diameter with measures on at least two independent samples per condition.

The smallest diameters are obtained for lecithin/PEG surfactants ratio w/w around 0.5.

These results demonstrate the complex influences of the different ingredient ratios on the LNP properties, such as their hydrodynamic diameter. A design of experiments is therefore used to rationalize the obtained results and better apprehend the LNP physicochemical behaviour.

3.5. Design of experiments

The 'one-variable-at-a-time' investigation (i.e. studying the response by changing one factor at a time, keeping all other factors at constant levels) is very time-consuming and may be difficult to perform when willing to understand the physicochemical behaviour of a system affected by numbers of factors [39]. In addition, it can lead to misinterpretations of the obtained results, since interactions cannot be clearly evidenced with such a strategy [39]. The methodology based on the design of experiments overcomes these issues, and present many more advantages [39]. This approach maximizes the number and quality of obtained information, while minimizing the required experimental effort, and is more and more used for both research and industrial purposes [39].

The use of this approach to further understand the impact of the different composition parameters on the LNP physicochemical properties is therefore straightforward. Four compositions factors completely describing the LNP system are investigated: aqueous buffer weight fraction (X_1), lipid mixture weight fraction (X_2), lipophilic surfactant and hydrophilic surfactant weight fractions (respectively noted X_3 and X_4). Two surfactants are used for the construction of the design of experiments (Myrj s100™ and Myrj s40™), but only results with Myrj s40™ (polyoxyethylene-40-stearate) will be presented and discussed here. The effects of the composition parameters on particle diameter and emulsion polydispersity index responses are evaluated. Particle diameter is a critical parameter for LNP accurate description, meanwhile LNP polydispersity reflects their physical stability: the more monodisperse a dispersion, the highest its colloidal (or physical) stability [21].

In such a complex physicochemical system, direct influence of each factor but also interactions between factors need to be considered, as exemplified by the relative proportion of the hydrophilic and lipophilic surfactants (Fig. 7). Full factorial designs are appropriate to evaluate main effects as well as interactions between factors, but they require carrying out a high number of experiments [39]. A D-optimal design, that can manage constraints imposed on the different composition factors, is thus used to reduce the number of experiments while keeping high information content. Second order interactions between factors are considered, but the influence of 3rd and superior order interactions are hypothesized to be negligible. Constraints are also imposed on the compositions factors to reduce the domain of study to formulations giving concentrated enough dispersions (weight fraction of dispersed phase >10%), and nanoparticles with sufficient surfactant concentrations to ensure consequent physical stability [21]. Then 32 design points are selected to minimize the variance associated with the estimates of the coefficients in the specified model. However, further trials are added to improve the model accuracy (repetition of most influent points, determined by leverage superior to 0.6 [40] and addition of complementary formulation trials). At the end, 82 trials are used to model two quantitative responses (particle diameter and emulsion polydispersity) (Fig. 8A).

To optimize the model accuracy for small particle size values, the LNP diameter response is expressed through its inverse. The model appears statistically significant since residuals nicely follow a normal plot (Fig. S2 in Supplementary information), the model presents a rather good regression coefficient (R^2 = 0.90) and a good reliability, reflected by the proximity of R^2 and $R^2_{adjusted}$ ($R^2_{adjusted} = 0.88$ [40]) (Fig. 8A). The accuracy of the model is tested by using 40 other experimental trials as tests. Fig. 8B displays the correlation plot between the experimental particle hydrodynamic diameter and the model-predicted data. Similar graph is available in the Supporting information for polydispersity (Fig. S3). A very good correlation is achieved between the model and experimental trials for LNP with diameters between 20 and 120 nm (<20% on nm-diameter size) (Fig. 8B and zoom). The diameter model is thus qualified and can be used for further optimisation procedure. The results obtained for the polydispersity model are less accurate (Fig. S3 in Supplementary information), and its use will be consequently limited to avoiding the choice of formulations with highly polydisperse population during optimisation process.

Further studies are performed to deeply qualify the diameter model accuracy, to precise the domain limits of the design of experiments, and to link the physicochemical parameters to physical stability. For that purpose, a 'one-variable-at-a-time' approach is used. Comparison between model-response data and measured values in supplementary experiments (i.e. which have not been used to build the model) is performed (Fig. 9). In addition, physical stability of the dispersions is evaluated by the quantitation of the evolution of the particle diameter after 4 months storage at room temperature ($T = 22 \pm 2$ °C), and conjointly presented in Fig. 9.

An increase of the PEG surfactant concentration reduces the LNP diameter (Fig. 9A), as previously demonstrated in Fig. 7. Two concentration ranges can be discerned: (i) a 'surfactant poor regime' for PEG surfactant weight below 150 mg, for which increasing the mass of the PEG surfactant leads to a dramatic diameter decrease; (ii) a 'surfactant rich regime', in which the sensitivity of LNP diameter upon addition of PEG is less pronounced [31]. The 'surfactant rich regime' (ii) corresponds to a zone of good correlation between the experimentally obtained particle diameter and the particle diameter predicted by the model, and the zone giving stable LNP dispersion after 4 months storage at room temperature (Fig. 9B). As LNP have a neutral surface charge, the PEG surfactant coverage is critical for preventing coalescence both in the emulsification step and for further colloidal stability [21]. A too poor PEG coverage (zone (i)) leads to poor correlation between the predicted and experimental data. In this range (weight PEG $\leqslant$ 150 mg), lipid nanoparticles cannot reach their saturated diameter during the emulsification step (5 min sonication) [21] and unstable formulations with particle size increasing with time are obtained, as shown in Fig. 9B.

A similar effect (two-zone domains) is observed when considering the total surfactants over lipids weight ratio (Fig. 9C). The investigated surfactant concentration range is nonetheless not low enough to observe a significant effect on the physical LNP stability. This stability is preserved up to surfactant/core ratio about 2.2 (Fig. 9D). At higher surfactant/core ratio, a destabilisation is observed. Stability is thus achieved when sufficient surfactant concentration is introduced for complete interface coverage (Fig. 9C). Yet, adding two much surfactants leads to the formation of micelles and mixed species in solution, which favour Ostwald ripening by facilitating lipid material solubilisation in the continuous phase (Fig. 9D) [9].

The influence of the two surfactants ratio is reported in Fig. 9E and F. It can be seen that stability is experimentally favoured for a mixture of both surfactants, in the range 1.5 < PEG surfactant/lecithin weight ratio < 6.6. In parallel, a good correlation between model-predicted and experimental data is observed for intermediate surfactant weight ratios. Both PEGylated chains and phospholipids therefore appear necessary at the LNP interface to ensure the particle colloidal stability. The presence of PEG surfactants is crucial in preventing LNP coalescence through efficient steric

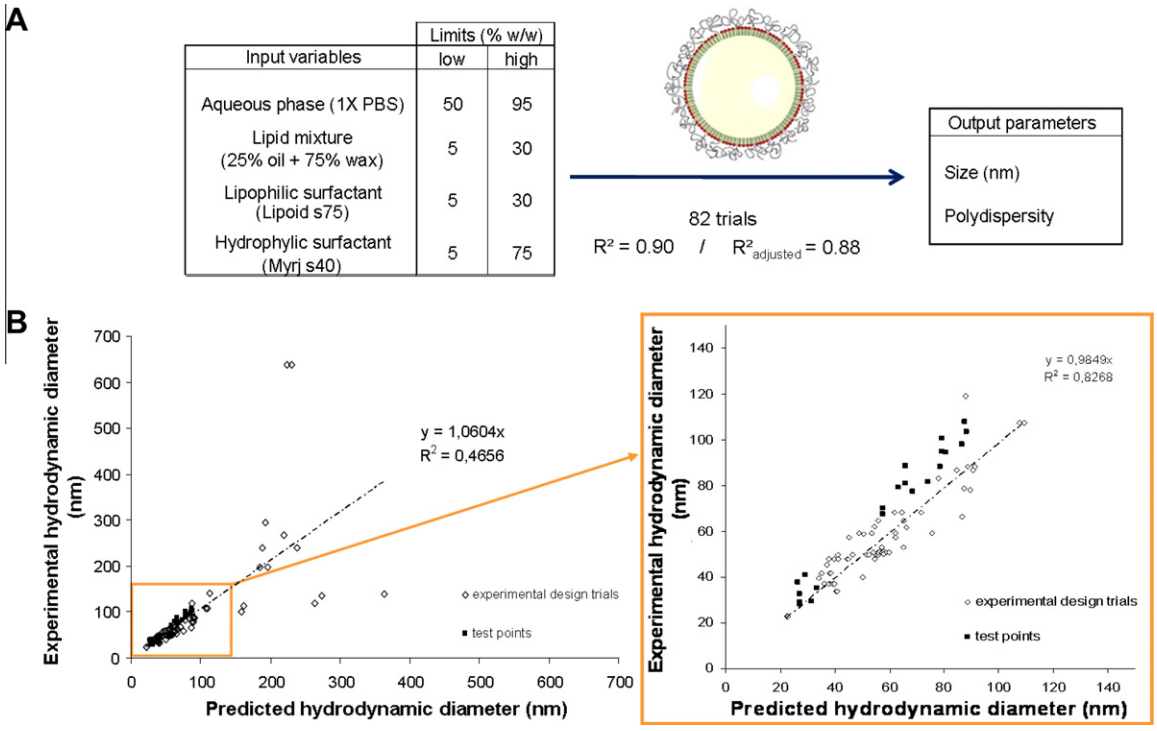

Fig. 8. Design of experiments description. (A) Four input variables have been selected: molar fractions of aqueous phase, core lipid mixture (with a 25% oil/75% wax composition), lipophilic surfactant (Lipoïd s75) and hydrophilic surfactant (Myrj s40). (B) Correlation plot between experimental and predicted particle hydrodynamic diameters.

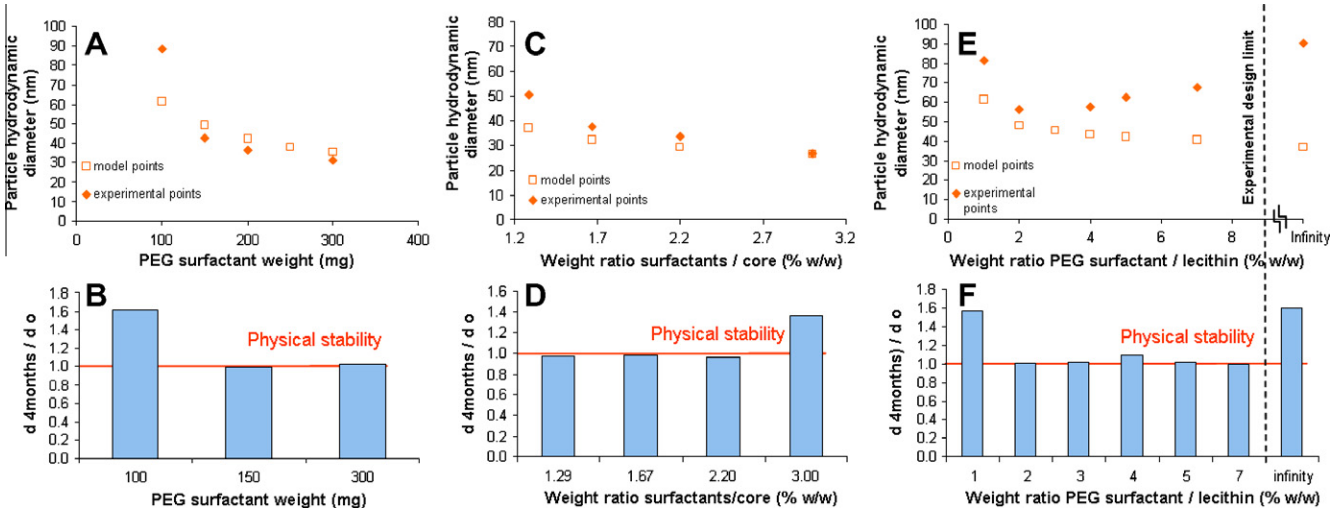

Fig. 9. Influence of the LNP formulation composition as predicted by the model based on the design of experiments, compared with results of supplementary experiments. (A and B) Influence of the PEG concentration. (C and D) Influence of the surfactants/lipids ratio. (E and F) Influence of the PEG/lecithin ratio. For each parameter, the upper graph displays the model and experimental (measured 1 day after LNP preparation) particle diameters. The lower graph displays the ratio of the experimental hydrodynamic diameter measured 1 day after LNP preparation (d_0) and 4 months after storage at 22 ± 2 °C ($d_{4\text{-months}}$). An increase of this ratio indicates a particle destabilisation. Formulations used (2 mL samples): (A and B) 200 mg NC75; X = 100, 150, 200, 250, 300 mg Myrj s40; 100 mg Lipoid s75 in Y = 1600, 1550, 1500, 1450, 1400 µL 1X PBS. (C and D) X = 200, 175,150, 125, 100 mg NC75; Y = 166, 187, 208, 229, 250 mg Myrj s40; Z = 33, 37, 42, 46, 50 mg Lipoid s75 in 1600 µL 1X PBS. (E and F) 200 mg NC75; X = 200, 175, 166, 160, 150, 133, 100, 50 mg Myrj s40; Y = 0, 25, 33, 40, 50, 66, 100, 150 mg Lipoid s75 in 1600 µL 1X PBS (X, Y, Z represent the variables in each experiment).

repulsion, while the particle surface is nearly neutral. Meanwhile, the presence of lecithin is critical to prevent Ostwald ripening, by favouring entropic stabilisation [21]. It can also promote intermediate membrane rigidity, lowering particle destabilisation by constituting an efficient barrier to mass transfer (reduction of Ostwald ripening) and to membrane fusion (reduction of coalescence) [21].

In all the cases explored (Fig. 9), the design of experiments model accuracy is good for formulations presenting a good physical stability. This is achieved roughly in the domain: $0.4 < X_1 < 0.9$, for a surfactants to core ratio of $(X_3 + X_4)/X_2 < 2$ and a lecithin to PEG surfactant ratio of $0.01 < X_3/X_4 < 5$. For too concentrated or too diluted formulations, LNP processing cannot be performed:

either viscosity problems ($X_1 < 0.4$) or too important foaming occur ($X_1 > 0.9$). The frontiers for the other parameters (X_2, X_3, X_4) are not so easy to define, because of the strong interplay between the different lipid and surfactant weight ratios (Figs. 7 and 9). However, it is clear that the presence of both surfactants in sufficient quantities is crucial for long-term LNP stability and for achieving small particle diameter, whereas an excess of surfactants could favour the formation of micelles, a factor of destabilization by Ostwald ripening. These results also underline that both the LNP core and shell composition play a crucial role in one very important property of the system: its colloidal stability. This stability relies on the choice of the ingredients, and every one is essential, as well as on their relative proportion in the final formulation. The use of sonication, a high energy process, is also very important, since it is the mean that allows the exploration of this quite wide range of composition domain, for which LNP nanoemulsions, nonthermodynamically stabilized systems, are kinetically stable [21]. The strong interplay between the LNP composition factors also demonstrate the benefit of using a design of experiments, using a multi-factorial approach, in order to propose in the future stable formulations with desired characteristics, such as defined particle diameters, dedicated to different applications.

4. Conclusions

New lipid nanoparticles have been designed based on low cost and human-approved excipients and manufactured by an easy, robust, and up-scalable process. This work has been focused on the physico-chemical characterization of these nanocarriers. The extreme resistance to lipid crystallization and the tuneable viscosity of the particle lipid core is demonstrated. LNP appear very similar to the already described structureless type (ii) NLC [11]. However, thanks to their manufacturing process and their composition, a wider range of particle diameters (30–200 nm), formulation viscosities (from fluid solutions to viscous gel formulations), and most important, far increased long-term stability (up to 12 months at 40 °C) are observed for the LNP system in comparison to previously described lipid carriers.

LNP should therefore present all the necessary characteristics for use as efficient contrast agent vehicle or drug nanocarriers, either for parenteral, topical or other routes. Their use as fluorescent tracers for *in vivo* tumour-targeted preclinical imaging has already been demonstrated whenever loaded with up to a few hundreds of fluorophores per particle [30,41]. Future studies will be focused on drug encapsulation and release, which will necessitate the encapsulation of more important payloads. Thanks to their core tuneable viscosity, LNP should avoid overcome the drug expulsion problem often encountered with lipid nanoparticles, and allow controlled kinetics of drug release.

Acknowledgments

This work is supported by the Commissariat à l'Energie Atomique et aux Energies Alternatives and the French National Research Agency (ANR) through Carnot funding and Contract No. ANR-08-PNANO-006-02. The authors thank P. Ozil for his help in analyzing the design of experiments, G. Marchand for his kind advices during manuscript redaction, and S. Derrough, C. Sourd, P. Sailler and L. Heux for support during DSC characterization.

Appendix A. Supplementary material

Supplementary data associated with this article can be found, in the online version, at doi:10.1016/j.jcis.2011.04.080.

References

[1] Y. Liu, H. Miyoshi, M. Nakamura, Int. J. Cancer 120 (2007) 2527.
[2] L. Zhang, F.X. Gu, J.M. Chan, A.Z. Wang, R.S. Langer, O.C. Farokhzad, Clin. Pharmacol. Ther. 33 (5) (2008) 761.
[3] V.P. Torchilin, V.P. Torchilin (Eds.), Nanoparticulates as Drug Carriers, Imperial College Press, London, 2006, p. 724.
[4] P. Simard, J.C. Leroux, C. Allen, O. Meyer, A.J. Domb, et al. (Eds.), Nanoparticles for Pharmaceutical Applications, American Scientific Publishers, 2007.
[5] S.M. Moghimi, E. Vega, M.L. Garcia, O.A.R. Al-Hanbali, K.J. Rutt, V.P. Torchilin (Eds.), Nanoparticulates as Drug Carriers, Imperial College Press, London, 2006.
[6] A. Wretlind, J. Parenter. Enter. Nutr. 5 (1981) 153.
[7] R.H. Müller, W. Mehnert, J.S. Lucks, C. Schwarz, A. Zur Mühlen, H. Weyhers, et al., Eur. J. Pharm. Biopharm. 50 (1995) 161.
[8] S.A. Wissing, O. Kayser, R.H. Müller, Adv. Drug Delivery Rev. 56 (2004) 1257.
[9] T. Tadros, P. Izquierdo, J. Esquena, C. Solans, Adv. Colloid Interface Sci. 108–109 (2004) 303.
[10] K. Westesen, H. Bunjes, M.J.H. Koch, J. Controlled Release 48 (1997) 223.
[11] R.H. Müller, M. Radtke, S.A. Wissing, Int. J. Pharm. 242 (2002) 121.
[12] R.H. Müller, K. Mäder, S.H. Gohla, Eur. J. Pharm. Biopharm. 50 (2000) 161.
[13] H. Bunjes, K. Westesen, M.J.H. Koch, Int. J. Pharm. 129 (1996) 159.
[14] A. Saupe, S.A. Wissing, A. Lenk, C. Schmidt, R.H. Müller, Biomed. Mater. Eng. 15 (2005) 393.
[15] M. Garcia-Fuentes, M.J. Alonso, D. Torres, J. Colloid Interface Sci. 285 (2005) 590.
[16] K. Jores, W. Mehnert, M. Drechsler, H. Bunjes, C. Johann, K. Mäder, J. Controlled Release 95 (2004) 217.
[17] S. Doktorovova, E.B. Souto, Expert Opin. Drug Delivery 6 (2009) 165.
[18] A. Lippacher, R.H. Müller, K. Mäder, Int. J. Pharm. 214 (2001) 9.
[19] W. Mehnert, K. Mäder, Adv. Drug Delivery Rev. 47 (2001) 165.
[20] A. Lippacher, R.H. Müller, K. Mäder, Int. J. Pharm. 196 (2000) 227.
[21] T. Delmas, A.C. Couffin, I. Texier, F. Vinet, P. Poulin, et al., Langmuir, in press, doi: 10.1021/la104221q.
[22] B. Abismail, J.P. Canselier, A.M. Wilhelm, H. Delmas, C. Gourdon, Ultrason. Sonochem. 6 (1999) 75.
[23] A. Lippacher, R.H. Müller, K. Mäder, Eur. J. Pharm. Biopharm. 53 (2002) 155.
[24] C. Mantel, A. Chandor, D. Gasparutto, T. Douki, M. Atta, et al., J. Am. Chem. Soc. 130 (2008) 16978.
[25] M.A. Maurer-Jones, J.K.G. Bantz, S.A. Love, B.I. Marquis, C.L. Haynes, Nanomedicine 4 (2009) 219.
[26] M.D. Joshi, R.H. Müller, Eur. J. Pharm. Biopharm. 71 (2009) 161.
[27] A.E. Nel, L. Mädler, D. Velegol, T. Xia, E.M.V. Hoek, P. Somasundaran, Nat. Mater. 8 (2009) 543.
[28] M. Howard, M. Jay, T.D. Dziublal, X. Lu, J. Biomed. Nanotechnol. 4 (2008) 133.
[29] J. Rossi, J.C. Leroux, K.M. Wasan (Eds.), Role of Lipid Excipients in Modifying Oral and Parenteral Drug Delivery, John wiley & Sons, Inc., Hoboken, New Jersey, USA, 2007.
[30] I. Texier, M. Goutayer, A. Da Silva, L. Guyon, N. Djaker, V. Josserand, et al., J. Biomed. Opt. 14 (2009) 054005.
[31] L. Taisne, P. Walstra, B. Cabane, J. Colloid Interface Sci. 184 (1996) 378.
[32] P.R. Smith, M.J.W. Pvey, J. Am. Oil Chem. Soc. 74 (1997) 169.
[33] K. Sato, Chem. Eng. Sci. 56 (2001) 2255.
[34] C. Freitas, R.H. Müller, Eur. J. Pharm. Biopharm. 47 (1999) 125.
[35] A. Zur Mülhen, C. Schwarz, W. Mehnert, Eur. J. Pharm. Biopharm. 45 (1998) 149.
[36] M. Bardet, M.F. Foray, J. Magn. Reson. 160 (2003) 157.
[37] A. Guillermo, G. Gerbaud, M. Bardet, Chem. Phys. Lipids 163 (2010) 309.
[38] M. Garcia-Fuentes, D. Torres, M. Martin-Pastor, M.J. Alonso, Langmuir 20 (2004) 8839.
[39] G.A. Lewis, D. Mathieu, R. Phan-Tan-Luu, Drugs and the Pharmaceutical Sciences, Marcel Decker, Inc., New York, 1999.
[40] J. Goupy, La méthodologie des plans d'expériences: optimisation du choix des essais & de l'interprétation des résultats, Paris, Dunod, 1988, p. 303.
[41] M. Goutayer, S. Dufort, V. Josserand, A. Royère, E. Heinrich, F. Vinet, et al., Eur. J. Pharm. Biopharm. 75 (2010) 137.